Proc. Indian Acad. Sci. (Math. Sci.) Vol. 116, No. 1, February 2006, pp. 97–119.

Formulation of the problem of sonic boom by a maneuvering aerofoil as a one-parameter family of Cauchy problems

S BASKAR and PHOOLAN PRASAD

Department of Mathematics, Indian Institute of Science, Bangalore 560 012, India
E-mail: prasad@math.iisc.ernet.in

MS received 28 February 2005; revised 29 November 2005

Abstract. For the structure of a sonic boom produced by a simple aerofoil at a large distance from its source we take a physical model which consists of a leading shock (LS), a trailing shock (TS) and a one-parameter family of nonlinear wavefronts in between the two shocks. Then we develop a mathematical model and show that according to this model the LS is governed by a hyperbolic system of equations in conservation form and the system of equations governing the TS has a pair of complex eigenvalues. Similarly, we show that a nonlinear wavefront originating from a point on the front part of the aerofoil is governed by a hyperbolic system of conservation laws and that originating from a point on the rear part is governed by a system of conservation laws, which is elliptic. Consequently, we expect the geometry of the TS to be kink-free and topologically different from the geometry of the LS. In the last section we point out an evidence of kinks on the LS and kink-free TS from the numerical solution of the Euler's equations by Inoue, Sakai and Nishida [5].

Keywords. Sonic boom; shock propagation; ray theory; elliptic equation; conservation laws; Cauchy problem.

1. Introduction

When an aircraft moves with a supersonic speed, two conical shock surfaces extending behind the aircraft from nose and tail are generated. The region between the two conical surfaces is the entire region of pressure disturbance at a given instant. The lower part of this pressure disturbance propagates from the aircraft to the ground. The leading shock front (let us call it LS) starting from the nose of the aircraft gives rise to a sudden pressure increase in the atmosphere. For a steady motion of the aircraft, the pressure disturbance in between the LS and the trailing shock (TS) decreases almost linearly across the disturbance till it reaches the TS in front of which the pressure falls below the atmospheric pressure. A sudden compression takes place at the TS and the pressure is restored to its atmospheric value. Thus the pressure disturbance far from the body develops N-shape which is commonly known as N-wave. An observer on the ground will recognize this pressure variation as a noise which starts with a bang and ends with another bang. This phenomenon of the noise with two bangs is called *sonic boom*. The loud noise of the sonic boom and the associated bangs are undesirable effects of supersonic flights in any locality which is not far away from the aircraft. The N-wave signature of a boom is modified to a U-wave signature in a focused boom produced by an accelerating aircraft (or more generally a maneuvering aircraft, figure 3 of [10]), for which the only available code is a very old one, PCBoom

3 by Crow [4]. Our main aim in this paper is to present a new mathematical formulation (i) to find full geometrical shape of the LS and TS with all finer details for an arbitrary motion (i.e., general maneuvering) of the aircraft and (ii) to calculate the full signature of the boom at any location far away from the aircraft. The method which we develop is computationally efficient.

Sonic boom had been anticipated in the early 50's of the 20th century even in early stages of supersonic flights of aircraft. Due to this unpleasant and destructive feature, an aircraft is restricted today to fly at supersonic speeds only across the oceans. This restriction clearly shows the importance of the study of sonic boom problem. Developments in the fundamental theory of sonic boom and the implementation to practical models took almost two decades but this field of research is still active (see [10]) and the particular issue of the JASA containing this paper and a large number of other papers dealing with the various aspects of sonic boom research till the end of the last century). An extensive literature survey shows that though menace of the sonic boom cannot be fully eliminated, the mathematical aspects of the problem need much more attention. This is mainly because, the commonly used codes developed so far use linear ray theory to start the solution and then use an approximate but a very elegant simple nonlinear theory (due to Whitham [13]) in which the amplitude is calculated along the linear rays. The results are fine as long as the problem can be described in two independent variables, for example, a steady two-dimensional case, but once three independent variables appear (say, x, y and t) as in the case of an unsteady two-dimensional case, the results using linear rays become inadequate since the nonlinear rays diffract significantly from the linear ones. Hence, the sonic boom problem produced by a maneuvering aircraft remains an open mathematical problem even today. Also, it is important to note [10] that while calculating sonic boom signature one needs to calculate the far-field solution, as the main aim in this problem is to find the pressure disturbance on the ground when a supersonic aircraft flies at a high distance from the ground level. In such cases it is expensive and sometimes may not be possible to go for a full numerical solution of the original gas dynamics equations [5,9]. So, we need approximate methods to take into account diffraction of nonlinear rays and which also reduces computational time. The new mathematical formulation of this problem presented here is restricted to two spatial dimensions but gives the full far-field sonic boom signature with finer geometrical features of the LS and TS. This simple formulation is valid also in the case of a maneuvering aerofoil – which is a challenging problem and is achieved in a ray coordinate system with just two independent variables instead of the original three independent variables x, y and t. The basis of formulation are two previous theories – a weakly nonlinear ray theory (WNLRT) [12] and a shock ray theory (SRT) [8] for a weak shock. For the role played by the two theories, it is crucial to understand the difference between a nonlinear wavefront (across which the flow variables are continuous) in the high frequency approximation and a shock front (§1.8 of [11]). Some of the equations of the two approximate theories are equivalent to the differential forms of a pair of exact geometrical results, namely kinematical conservation laws (KCL) by Morton, Prasad and Ravindran [7]. All these basic results are available in a book by Prasad [11]. The SRT is ideally suited in dealing with the sonic boom problem since

(i) it has been shown that it gives results which agree well with known exact solutions and experimental results [6],
(ii) it gives a sharp geometry of the shock and many details of its finer geometrical features [8],

(iii) results obtained by it also agree well with those obtained by numerical solutions of full Euler equations [2] and
(iv) it takes considerably less computational time (say less than 10%) compared to computation by the original Euler equations.

As described in the next section, the far-field sonic boom satisfies high frequency approximation, and hence its signature in between the LS and TS is generated by a one-parameter family of nonlinear wavefronts Ω_ζ starting from the various points P_ζ on the upper and lower surfaces of the aerofoil separated by a linear wavefront Ω_G from a point P_G where the tangent to the aerofoil surface is parallel to the camber line. Our mathematical formulation is in terms of one-parameter family of Cauchy problems for a system of conservation laws (i.e., WNLRT) governing the evolution of this one-parameter family of nonlinear wavefronts. The system changes its nature from hyperbolic to elliptic as the parameter ζ goes from one sub-interval to another sub-interval on the two sides of $\zeta = G$. The formulation also contains two Cauchy problems for another system of conservation laws (SRT) governing the evolution of the LS and the TS, the system is hyperbolic for the LS and is elliptic for the TS. We hope to report in future many interesting physical features of the sonic boom through some theoretical results and extensive computation with the help of our formulation. These computations will require not only new numerical schemes but also a lot of trials with different schemes for the cases when the system is elliptic. Hence, we present only the mathematical formulation in this paper with just a few simple numerical results at the end. Those involved in calculating sonic boom signature from a maneuvering aircraft, will notice a simplicity in our method, enormous time-saving in computation and evidence of new results such as *the trailing shock must always be free from kinks* and *the leading shock may have a different topological shape with two or more kinks on it*. Unlike the previous methods, our method fully takes into account the nonlinearity of the evolution equations from the very beginning. It does not take linear solution to start the solution for small time and then builds nonlinearity on linear solution.

2. Formulation of the problem

Consider a two-dimensional unsteady flow produced by a maneuvering supersonic aerofoil whose leading edge (or the nose) is moving along a curved path. We assume the ambient unperturbed medium to be uniform and at rest. Our formulation is based on four assumptions:

Assumption A.1. The aerofoil is thin.

Assumption A.2. The length of the aerofoil, i.e., its camber length $\bar{d}$ is small compared to the distance L of the point of observation of the sonic boom from the aerofoil.

Assumption A.3. The camber length $\bar{d}$ is small compared to the radius of curvature R of the path of the leading nose.

Assumption A.4. The camber line is aligned along the direction of motion of the aerofoil.

Due to Assumptions A3 and A4, we can assume the camber line to be approximately coincident with the path of the leading edge or the nose of the aerofoil.

We denote the coordinate system in the plane of the motion of the aerofoil by $(\bar{x}, \bar{y})$ and the time by $\bar{t}$. The appropriate time scale for our problem is $T = L/a_0$, where a_0 is the constant sound velocity in the uniform ambient medium. We introduce the non-dimensional variables as follows:

$$t = \frac{\bar{t}}{T}, \quad x = \frac{\bar{x}}{L}, \quad y = \frac{\bar{y}}{L}, \quad d = \frac{\bar{d}}{L},$$

where a quantity with a bar denotes a dimensional variable. Throughout our work, all the independent variables we use are non-dimensional in the above sense.

To describe the geometry of the aerofoil, we introduce a local rectangular coordinate system (x', y') with the origin O' at the nose of the aerofoil such that at any time t, $O'x'$ is in the direction tangential to the aerofoil path and $O'y'$ is perpendicular to it. Let us denote the curved path of the aerofoil traced by the nose of the aerofoil in the (x, y)-plane by $(x = X_0(t), y = Y_0(t))$. Every point on the surface of the aerofoil moves with the same velocity $(\dot{X}_0(t), \dot{Y}_0(t))$ making an angle, say $\psi(t)$ with the direction of the x-axis, so that

$$\tan\psi = \frac{\dot{Y}_0(t)}{\dot{X}_0(t)}. \tag{2.1}$$

Thus, the aerofoil moves in the direction $(\cos\psi, \sin\psi)$ of the $O'x'$ axis (figure 2.1). Hence,

$$\begin{aligned} x' &= \langle(\cos\psi, \sin\psi), (x - X_0(t), y - Y_0(t))\rangle \\ &= x\cos\psi + y\sin\psi - \mathcal{X}_0(t), \end{aligned} \tag{2.2}$$

$$\begin{aligned} y' &= \langle(-\sin\psi, \cos\psi), (x - X_0(t), y - Y_0(t))\rangle \\ &= -x\sin\psi + y\cos\psi - \mathcal{Y}_0(t), \end{aligned} \tag{2.3}$$

where

$$\mathcal{X}_0 = X_0\cos\psi + Y_0\sin\psi, \quad \mathcal{Y}_0 = -X_0\sin\psi + Y_0\cos\psi. \tag{2.4}$$

Due to Assumption A3, we can take the camber line to be straight and coincident with the $O'x'$-axis between $x' = -d$ and $x' = 0$ (due to the Assumption A4, the line $O'x'$ deviates from the path only over a distance large compared to the camber length d). We denote the upper and the lower surfaces of the aerofoil by

$$(x' = \zeta, \quad y' = b_u(\zeta)) \quad \text{and} \quad (x' = \zeta, \quad y' = b_l(\zeta)), \quad -d \le \zeta \le 0 \tag{2.5}$$

respectively. We assume that $b_u(\zeta) \ge 0, b_l(\zeta) \le 0, b_u''(\zeta) \le 0, b_l''(\zeta) \ge 0$ for $-d \le \zeta \le 0$. In addition, we also assume that $b_u'(-d) > 0$, $b_u'(0) < 0$, $b_l'(-d) < 0$ and $b_l'(0) > 0$, so that the nose and the tail of the aerofoil are not blunt.

We denote a point on the surface of the aerofoil by P_ζ. The position of this point at a given time t in the fixed (x, y)-plane is $(X_\zeta(t), Y_\zeta(t))$ where

$$X_\zeta(t) = X_0(t) + \zeta\cos\psi(t) - b_u(\zeta)\sin\psi(t), \tag{2.6}$$

$$Y_\zeta(t) = Y_0(t) + \zeta\sin\psi(t) + b_u(\zeta)\cos\psi(t), \tag{2.7}$$

where $-d \le \zeta \le 0$ and the path of P_0 i.e., the nose of the aerofoil is $(X_0(t), Y_0(t))$ as stated earlier.

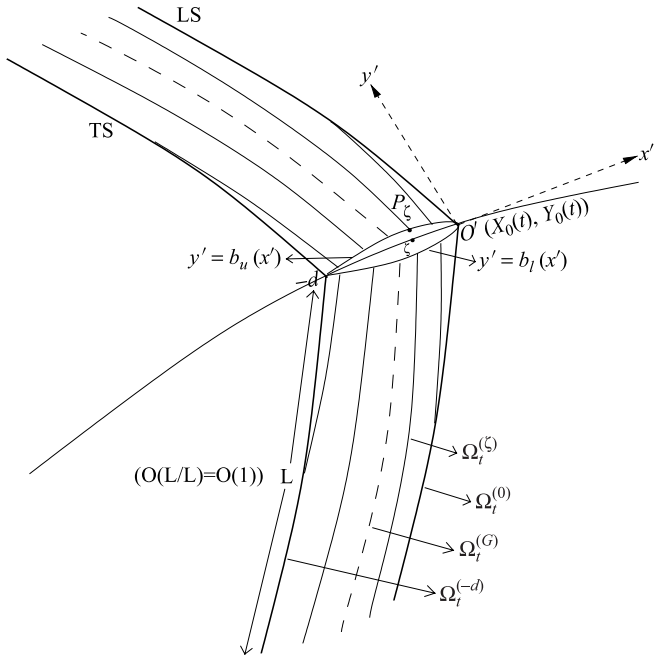

Figure 2.1. Sonic boom produced by the upper and lower surfaces: $y' = b_u(x')$ and $y' = b_l(x')$ respectively. The boom produced by either surface consists of a one-parameter family of nonlinear wavefronts $\Omega_t^{(\zeta)}$, $-d < \zeta < 0$ (shown by thin lines) and is bounded by a leading shock LS and a trailing shock TS. The linear wavefront $\Omega_t^{(G)}$ is shown by a broken line.

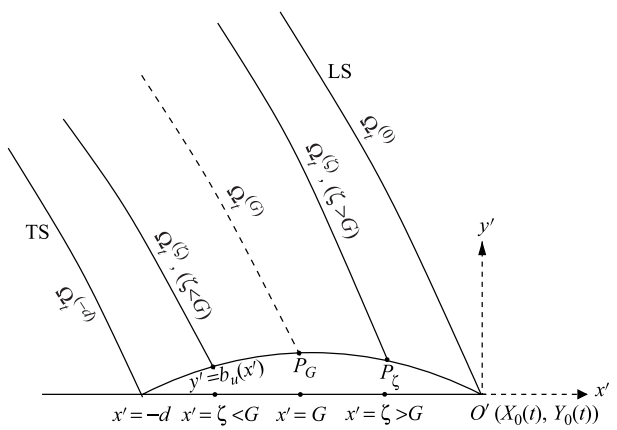

Figure 2.2. An enlarged version of the upper part of figure 2.1 near the aerofoil.

In figure 2.1, we show the geometry of the aerofoil and the sonic boom produced by it at any time t. The sonic boom produced either by the upper surface or the lower surface consists of a leading shock LS: $\Omega_t^{(0)}$ and a trailing shock TS: $\Omega_t^{(-d)}$, which are shown by thick lines in the figure. The sonic boom produced by the upper and the lower surfaces spread slowly (figure 2.1). Figure 2.2 shows an enlarged version of the upper part of

figure 2.1 near the aerofoil. Since $d = \bar{d}/L =: \epsilon \ll 1$, the flow in the sonic boom between LS and TS is contained in a thin strip for which the ratio of the width to its length is of the order of ϵ, so that this flow satisfies high frequency assumption. The aerofoil is thin i.e., the ratio of the thickness $\max_{-d<\zeta<0}(b_u(\zeta) - b_l(\zeta))$ of the aerofoil to d is also small and is assumed to be of $O(\epsilon)$, which implies that the amplitude of the disturbance in the sonic boom is small. Thus, the high frequency and small amplitude assumption of chapter 4 of [11] is satisfied and the flow in the boom between LS and TS can be characterized by one-parameter family of weakly nonlinear wavefronts $\Omega_t^{(\zeta)}$, $\{-d < \zeta < 0, \zeta \neq G\}$ originating from the various points P_ζ on the aerofoil. We shall define G later. To be more specific, we discuss only the sonic boom produced by the upper surface and in this paper P_ζ is a point on the upper surface as seen in figure 2.2. Thus, the nonlinear wavefront at a given time t starting from a point P_ζ on the upper surface of the aerofoil is $\Omega_t^{(\zeta)}$, $\{-d < \zeta < 0, \zeta \neq G\}$. By $\Omega_t^{(0)}$, we denote the leading shock front LS (note that the nonlinear wavefront starting from the leading edge P_0 is immediately annihilated by the LS and disappears from the flow). Similarly, we denote the trailing shock TS by $\Omega_t^{(-d)}$.

Nonlinear wavefronts produced from points on the front portion of the aerofoil start interacting with the LS and those from the points near the trailing edge do so with the TS, and after interaction they keep on disappearing continuously from the flow. These two sets, one interacting with the LS and another interacting with the TS are separated by a linear wavefront $\Omega_t^{(G)}$, which is explained at the end of §3. Note that figure 2.2 is simply an enlarged version of figure 2.1 near the aerofoil. Actually the high-frequency approximation is not valid in a neighborhood of the aerofoil and the flow is far more complex. We have mentioned in the beginning of the introduction that the signature of a boom produced by a maneuvering aerofoil is not a N-wave but a U-wave. A difference in the rates of interactions of the nonlinear wavefronts from the front and rear parts with the LS and TS respectively will produce a difference in the signature of the boom. We would like to examine in subsequent papers whether our theory is able to produce U-shape (and some other shapes also) of the signature.

Our objective in this work is to develop a ray theoretical method based on a weakly nonlinear ray theory (WNLRT) to calculate the nonlinear wavefronts $\Omega_t^{(\zeta)}$ $\{-d < \zeta < 0, \zeta \neq G\}$, ($G$ to be defined later) and a shock ray theory (SRT) to calculate the shock fronts LS and TS produced by a supersonic maneuvering aerofoil. An advantage of WNLRT and SRT theories is that the amplitude of the perturbation on $\Omega_t^{(\zeta)}$ is calculated simultaneously with the geometry of $\Omega_t^{(\zeta)}$. We describe the ray coordinate system and the basic equations for the calculation of each $\Omega_t^{(\zeta)}$ in the next section and derive the Cauchy data on a datum curve in the ray coordinate plane in §4. The introduction of the ray coordinate system (ξ, t) is such that the datum curve for calculation of each $\Omega_t^{(\zeta)}$, $-d \leq \zeta \leq 0$ is the same, namely $\xi + t = 0$.

3. Ray coordinate system

Let us now introduce a ray coordinate system (ξ, t) for $\Omega_t^{(\zeta)}$, where $t =$ constant represents the position of $\Omega_t^{(\zeta)}$ at the time t and $\xi =$ constant is a ray associated with the successive positions of $\Omega_t^{(\zeta)}$. As mentioned earlier, we restrict ourselves only to the upper surface of the aerofoil unless stated explicitly.

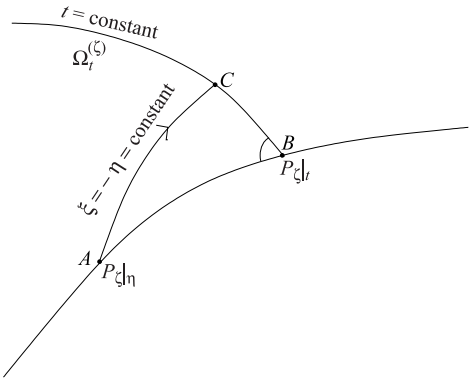

Figure 3.1. A formulation of the ray coordinate system (ξ, t) for $\Omega_t^{(\zeta)}$. AB represents the path of a fixed point P_ζ on the aerofoil. A and B are the positions of P_ζ at times η and t respectively, $\eta < t$.

When $\Omega_t^{(\zeta)}$ propagates in a uniform isotropic medium at rest, the rays are orthogonal to the successive positions of it. The front $\Omega_t^{(\zeta)}$ at a given time t can be obtained by Fermat's method of wavefront construction i.e., the line joining the tips of the rays at time t in the (x, y)-plane starting from all positions $P_\zeta|_\eta$ of P_ζ at times $\eta < t$ as shown in figure 3.1. The ray velocity will depend on the type of the front $\Omega_t^{(\zeta)}$, that is whether it is a linear or a nonlinear wavefront for $-d < \zeta < 0$ or whether it is a shock front for $\zeta = 0, -d$.

For a front $\Omega_t^{(\zeta)}$, $-d \le \zeta \le 0$, the ray coordinate system (ξ, t) is such that $\xi =$ constant is a ray. We note that a ray associated with $\Omega_t^{(\zeta)}$ can be identified by the starting point $P_{\zeta|\eta}$ of the ray at time η. Hence, as shown in figure 3.1, we choose

$$\xi = -\eta, \quad \eta \le t. \tag{3.1}$$

As $t \to \infty$ we get the full ray as the front $\Omega_t^{(\zeta)}$ moves away to infinity. Note that we shall have different ray coordinates (ξ, t) for different fronts $\Omega_t^{(\zeta)}$, i.e., for different values of ζ satisfying $-d \le \zeta \le 0$. For this choice of ξ, the variable ξ increases along $\Omega_t^{(\zeta)}$ as we move away from the aerofoil i.e., the curve $\Omega_t^{(\zeta)}$ is described in the positive sense so that the unit normal to $\Omega_t^{(\zeta)}$ points in the direction of propagation of $\Omega_t^{(\zeta)}$. For a front starting from the lower surface of the aerofoil, we take ξ of the ray coordinate system (ξ, t) to be

$$\xi = \eta, \quad \eta \le t. \tag{3.2}$$

In this case ξ increases as we move towards the aerofoil on $\Omega_t^{(\zeta)}$ in order that the unit normal to $\Omega_t^{(\zeta)}$ points in the direction of propagation of $\Omega_t^{(\zeta)}$.

We assume the medium to be a polytropic gas with equilibrium state: gas density $\bar{\rho} = \bar{\rho}_0$, velocity $\bar{\mathbf{q}} = \mathbf{0}$ and pressure $\bar{p} = \bar{p}_0$. The sound velocity a (note that there is no bar on a even though it is not non-dimensional) in the medium is given by $a^2 = \gamma \bar{p}/\bar{\rho}$, where γ is the ratio of specific heats. In high-frequency small amplitude approximation, the perturbations in the flow variables on any one of $\Omega_t^{(\zeta)}$, $-d \le \zeta \le 0$, can be expressed in terms of an amplitude $\tilde{w}$ as follows:

$$\bar{\rho} = \bar{\rho}_0 + \left(\frac{\bar{\rho}_0}{a_0}\right)\tilde{w}, \ \bar{\mathbf{q}} = (n_1\tilde{w}, n_2\tilde{w}), \ \bar{p} = \bar{p}_0 + \bar{\rho}_0 a_0 \tilde{w},$$

where $\mathbf{n} = (n_1, n_2)$ is the unit normal of the front $\Omega_t^{(\zeta)}$ (wavefront or shock front) and $\tilde{w}/a_0 = O(\epsilon)$, with $0 < \epsilon \ll 1$ and a_0 is the sound velocity in the equilibrium state. We introduce the non-dimensional variables

$$\rho = \bar{\rho}/\bar{\rho}_0, \quad \mathbf{q} = \bar{\mathbf{q}}/a_0, \quad p = \bar{p}/(\gamma \bar{p}_0), \quad w = \tilde{w}/a_0$$

in the physical quantities defined above to get

$$\rho = 1 + w, \quad \mathbf{q} = \mathbf{n}w, \quad p = \frac{1}{\gamma} + w. \tag{3.3}$$

Note that w here is w/a_0 in (6.1.1) of Prasad [11], but is same as w of Baskar and Prasad [2]. w is a small quantity of the order ϵ and represents excess of the density over the (nondimensional) density having value 1 in the medium in which the boom propagates. In the compression part of the boom (which we show to be in the front part) $w > 0$ and in the expansion part $w < 0$.

The Mach number m of the nonlinear wavefront is defined as the ratio of its normal velocity to the sound velocity in the ambient medium and is given by

$$m = 1 + \frac{\gamma + 1}{2} w. \tag{3.4}$$

The system of conservation laws governing the evolution of each $\Omega_t^{(\zeta)}$, $-d < \zeta < 0$, $\zeta \neq G$, are the equations of the WNLRT given by

$$(g \sin\theta)_t + (m \cos\theta)_\xi = 0, \quad (g \cos\theta)_t - (m \sin\theta)_\xi = 0, \tag{3.5}$$

$$(g(m-1)^2 e^{2(m-1)})_t = 0, \tag{3.6}$$

where g is the metric associated with the variable ξ (i.e., $g\mathrm{d}\xi$ is an element of length along $\Omega_t^{(\zeta)}$).

The value of $w|_{\text{shock}}$ at the LS or TS at any time t is the value of w on the nonlinear wavefront $\Omega_t^{(\zeta)}$ which interacts with the shock at that time. This nonlinear wavefront is identified by a particular value $\zeta(t)$ of ζ and $\lim_{t\to\infty} \zeta(t) = G$. The Mach number M of the LS (or TS) is the mean of the Mach number m on the nonlinear wavefront just behind the LS (or just ahead of the TS) and that of the wavefront on the other side where $w = 0$ and therefore is given in terms of $w|_{\text{shock}}$ by

$$M = 1 + \frac{\gamma + 1}{4} w\bigg|_{\text{shock}}. \tag{3.7}$$

We introduced a ray coordinate system (ξ, t) also for the shock fronts $\Omega_t^{(0)}$ and $\Omega_t^{(-d)}$ by the same definition (3.1) and (3.2) for the upper and lower surfaces of the aerofoil respectively. However, the rays used for a shock are shock rays. We remind once more that a ray coordinate system is different for different moving curves and hence (ξ, t)-coordinate system depends on ζ, $-d \leq \zeta \leq 0$. In this coordinate system t is the actual time but ξ is different for different $\Omega_t^{(\zeta)}$. A system of conservation form of the equations governing the evolution of LS and TS are [2]

$$(G \sin\Theta)_t + (M \cos\Theta)_\xi = 0, \ (G \cos\Theta)_t - (M \sin\Theta)_\xi = 0, \tag{3.8}$$

$$(G(M-1)^2 e^{2(M-1)})_t + 2M(M-1)^2 e^{2(M-1)} GV = 0, \tag{3.9}$$

$$(GV^2 e^{2(M-1)})_t + GV^3(M+1)e^{2(M-1)} = 0, \tag{3.10}$$

where $\mathbf{N} = (\cos\Theta,\ \sin\Theta)$ is the unit normal to the shock front and

$$V = \frac{\gamma+1}{4}\{\langle \mathbf{N}, \nabla\rangle w\}\Big|_{\text{shock front}} \tag{3.11}$$

in which the normal derivative $\langle \mathbf{N}, \nabla\rangle w$ is first evaluated in the region behind the LS for $\zeta = 0$ and from the region ahead of the TS for $\zeta = -d$ and then the limit is taken as we approach the shock.

We note that since $\eta \to t$, $B \to A$ in figure 3.1 and ξ has been chosen to be η, the point $(\xi = -t, t)$ in the ray coordinate plane (see figure 4.2) correspond to the point $P_\zeta|_t$. Hence as t varies, the points on the line $\xi + t = 0$ represent the successive positions of a fixed point P_ζ on the aerofoil. Thus, in the (ξ, t)-plane, the point of intersection of $\Omega_t^{(\zeta)}$ and the aerofoil surface $y' = b_u(\zeta)$ lies on the line $\xi + t = 0$. In the next section, we shall use the inviscid fluid flow condition on the boundary of the aerofoil to derive the Cauchy data on the boundary line $\xi + t = 0$ for systems (3.5) and (3.6). Similarly, we shall derive Cauchy data for systems (3.8)–(3.10) on the line $\xi + t = 0$.

For a simple, smooth and convex aerofoil, we shall show in the next section that w continuously increases from a negative value at P_{-d} to a positive value at P_0 attaining value zero at a point P_G, where $b_u(\zeta)$ is maximum. Thus, $m = 1$ on $\Omega_t^{(G)}$, which becomes a linear wavefront. Equation (3.6) is not valid at $m = 1$ and hence the evolution of $\Omega_t^{(G)}$ is obtained by the linear ray equations. The nonlinear wavefronts $\Omega_t^{(\zeta)}$ ahead of $\Omega_t^{(G)}$ (i.e., those for $G < \zeta < 0$) interact gradually with the LS and those behind $\Omega_t^{(G)}$ interact in a similar way with TS. Thus, individual nonlinear wavefronts $\Omega_t^{(\zeta)}$ gradually disappear from the flow field and ultimately as t tends to infinity the sonic boom signature would consist of the LS, TS and the nonlinear wavefronts produced by points in an immediate neighborhood of $(G, b_u(\zeta))$ on the aerofoil.

Before closing this section, we make a precise statement of the Assumptions A1 to A3. The thin aerofoil Assumption A1 is

$$O\left\{\frac{\max_{-d<\zeta<0} b_u(\zeta)}{d}\right\} = O\left\{\frac{\max_{-d<\zeta<0}(-b_l(\zeta))}{d}\right\} = O(\epsilon), \tag{3.12}$$

which implies $|b_u'(\zeta)| \ll 1$ and hence (see eq. (4.9) in the next section for the value on the aerofoil)

$$w = O(\epsilon). \tag{3.13}$$

For Assumptions A2 and A3, we take

$$d = \frac{\bar{d}}{L} = O(\epsilon), \quad \frac{\bar{d}}{R} = O(\epsilon), \quad \text{i.e., } L/R = O(1). \tag{3.14}$$

4. Derivation of the Cauchy data on the line $\xi + t = 0$

In this section, we derive the Cauchy data for the system of equations (3.5) and (3.6) of the nonlinear ray theory for the evolution of the nonlinear wavefronts $\Omega_t^{(\zeta)}$ ($-d < \zeta < G$ and $G < \zeta < 0$), and the Cauchy data for the system of equations (3.8)–(3.10) of the shock ray theory for the evolution of the shock front TS: $\Omega_t^{(-d)}$ from the upper surface of

the aerofoil (the Cauchy data for the above systems for $\Omega_t^{(\zeta)}$ originating from the lower surface of the aerofoil can be derived similarly on the line $\xi = t$). These are obtained from the condition that the normal velocity of an inviscid fluid on the surface of the aerofoil is same as the normal velocity of the surface at that point.

We define a function $f \equiv f(x, y, t)$ as

$$f(x, y, t) = y' - b_u(x'), \quad -d \le x' \le 0, \tag{4.1}$$

where x' and y' are given as functions of x, y and t by (2.2) and (2.3). Then from (2.5), the equation of the upper surface of the aerofoil is given by the equation

$$f(x, y, t) = 0, \quad -d \le x' \le 0. \tag{4.2}$$

A point P_ζ fixed on this surface moves with the velocity $(\dot{X}_0, \dot{Y}_0)$ and hence equating the normal velocity $(\dot{X}_0 f_x + \dot{Y}_0 f_y)/|\nabla f|$ of the moving surface $f(x, y, t) = 0$ to the normal component $q_n = (q_1 f_x + q_2 f_y)/|\nabla f|$ of the fluid velocity $\mathbf{q} = (q_1, q_2)$, we get the condition $q_1 f_x + q_2 f_y = \dot{X}_0 f_x + \dot{Y}_0 f_y$ on the upper surface (4.2). Using (2.2) and (2.3), we get $f_x = -\sin\psi - b_u'(\zeta)\cos\psi$, $f_y = \cos\psi - b_u'(\zeta)\sin\psi$, $-d \le \zeta \le 0$, so that this condition reduces to

$$(q_2\cos\psi - q_1\sin\psi) - (q_1\cos\psi + q_2\sin\psi)b_u'(\zeta) + b_u'(\zeta)\sqrt{\dot{X}_0^2 + \dot{Y}_0^2} = 0. \tag{4.3}$$

Mach angle is a well-known term in gas dynamics (see page 260 of [3]). In context with an unsteady motion of the type considered here, we define the Mach angle ϕ (see figure 4.1) to be the angle which the nonlinear wavefront $\Omega_t^{(\zeta)}$ makes with the stream line which on the aerofoil is in the tangent direction TP_ζ of the aerofoil surface. The tangent $P_\zeta T$ makes an angle $\phi_1 = \tan^{-1}\{b_u'(\zeta)\}$ with the line $P_\zeta x''$ parallel to the local coordinate axis $O'x'$, which itself makes an angle ψ with the line $P_\zeta x$ parallel to the original x-axis. In a frame of reference instantaneously coincident with the aerofoil, the fluid velocity at the point P_ζ consists of the velocity $(\dot{X}^2 + \dot{Y}^2)^{\frac{1}{2}}$ + a quantity of the order of w along $x''P_\zeta$. For simplicity in this paper, we neglect this quantity of the order of w. Its inclusion any way does not affect the results (4.13)–(4.15), which will be discussed in a subsequent paper. The sine of the Mach angle ϕ at P_ζ is equal to the ratio of the normal velocity m

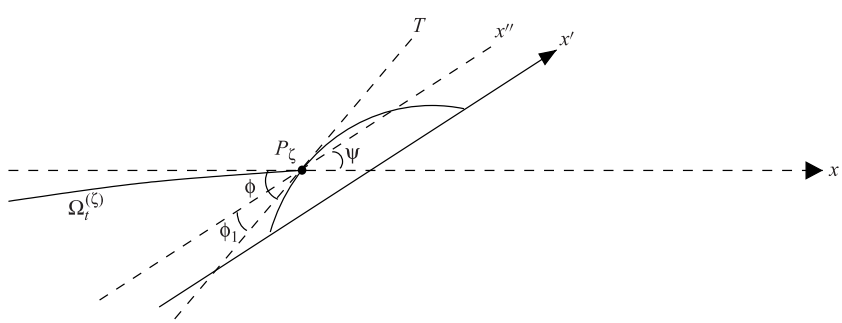

Figure 4.1. Figure showing the nonlinear wavefront $\Omega_t^{(\zeta)}$ making an angle ϕ with the stream direction TP_ζ on the aerofoil. Note that the dotted horizontal line is not the x-axis but is only in the direction of the x-axis

(given by (3.4)) of the nonlinear wavefront to the fluid speed $(\dot{X}_0^2 + \dot{Y}_0^2)^{1/2}$, relative to the aerofoil, at the fixed point P_ζ on the aerofoil i.e.,

$$\sin\phi = \frac{1 + (\gamma+1)w/2}{\sqrt{\dot{X}_0^2 + \dot{Y}_0^2}}. \tag{4.4}$$

Now we go back to figure 3.1, where the limiting direction of AB as $\eta \to t$ is the direction $P_\zeta x''$ and hence the $\angle ABC = \phi - \phi_1$ We also note that if B and C correspond to ξ and $\xi + \delta\xi$, then (due to choice (3.1)) for small $t - \eta = -\delta\xi$, $BC \simeq g\delta\xi$ and $AB \simeq \left|\sqrt{\dot{X}^2 + \dot{Y}^2}(t-\eta)\right| = \sqrt{\dot{X}_0^2 + \dot{Y}_0^2}\delta\xi$ (note $\delta\xi = -\delta\eta$), so that

$$g\delta\xi = \frac{BC}{AB}AB = \delta\xi\sqrt{\dot{X}_0^2 + \dot{Y}_0^2}\cos(\phi - \phi_1).$$

Hence, the value of g (with choice (3.1) for ξ) at the point of intersection of $\Omega_t^{(\zeta)}$ and the upper surface of the aerofoil is

$$g(\xi, t = -\xi) = \sqrt{\dot{X}_0^2 + \dot{Y}_0^2}\cos(\phi - \phi_1) = g_0(\xi), \text{ (say)}. \tag{4.5}$$

The unit normal to the nonlinear wavefront i.e., the direction of AC in figure 3.1 makes an angle $\theta = (\pi/2) - (\phi - \phi_1) + \psi$ with the x-axis and hence its direction $\mathbf{n}$ is given by

$$\mathbf{n} = (n_1, n_2) = (\sin(\phi - \psi - \phi_1), \cos(\phi - \psi - \phi_1)). \tag{4.6}$$

Perturbation of ρ, $\mathbf{q}$ and p on a nonlinear wavefront $\Omega_t^{(\zeta)}$ is given by (3.3) with the above expression for $\mathbf{n}$. Substituting it in the boundary condition (4.3), we get

$$w\{\cos(\phi - \phi_1) - \sin(\phi - \phi_1)b_u'(\zeta)\} + \sqrt{\dot{X}_0^2 + \dot{Y}_0^2}b_u'(\zeta) = 0 \text{ on } \xi + t = 0. \tag{4.7}$$

We note in figure 4.1 that ϕ_1 is the angle which the tangent $P_\zeta T$ makes with the flight direction i.e., $P_\zeta x''$ axis. This angle is small and of the same order as $b'(\zeta)$ for a thin aerofoil. In fact,

$$\phi_1 \simeq \tan\phi_1 = b_u'(\zeta) = O(\epsilon). \tag{4.8}$$

Hence, retaining terms only up to first order in $b_u'(\zeta)$, we get from (4.7)

$$w\cos\phi + \sqrt{\dot{X}_0^2 + \dot{Y}_0^2}b_u'(\zeta) = 0 \quad \text{on } \xi + t = 0. \tag{4.9}$$

Equations (4.4) and (4.9) are two relations at a point where $\Omega_t^{(\zeta)}$ meets the upper surface of the aerofoil i.e., at the point P_ζ. Solving these two equations for w and ϕ, we get the Mach angle ϕ and the amplitude w of the perturbation at P_ζ. Eliminating ϕ from these two relations, we get

$$w^2\left\{\dot{X}_0^2 + \dot{Y}_0^2 - \left(1 + \frac{\gamma+1}{2}w\right)^2\right\}$$
$$= \{\dot{X}_0^2 + \dot{Y}_0^2\}^2[-b_u'(\zeta)]^2 = 0, \text{ on } \xi + t = 0, \tag{4.10}$$

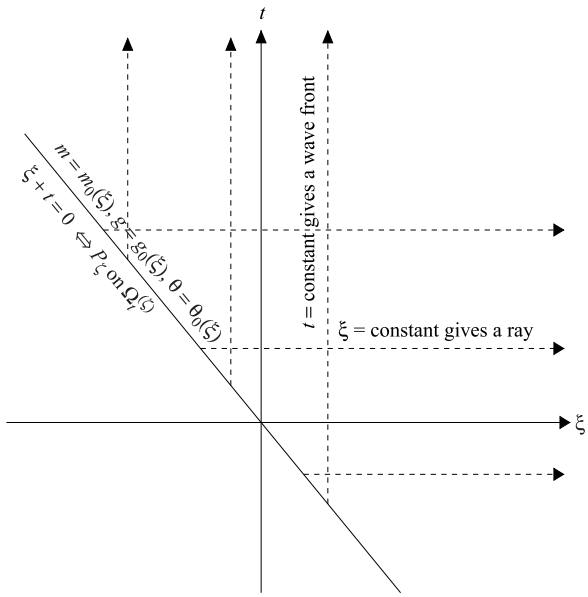

Figure 4.2. The successive positions of a fixed point P_ζ on the aerofoil corresponds to points on $\xi + t = 0$, where Cauchy data is prescribed. Solution domain is $\xi + t > 0$.

which gives $w(\xi, t = -\xi) = w_0(\xi)$, i.e., w at P_ζ at any time t. Since the nonlinear ray theory and the shock ray theory used here are both for small amplitude, a second order correction in w from (4.10) is not necessary. This gives on $\xi + t = 0$,

$$w(\xi, t = -\xi) = -\frac{(\dot{X}_0^2 + \dot{Y}_0^2) b_u'(\zeta)}{(\dot{X}_0^2 + \dot{Y}_0^2 - 1)^{1/2}} =: w_0(\xi), \text{ say, } -d \le \zeta \le 0. \quad (4.11)$$

The negative sign is appropriate for the upper surface. For lower surface of the aerofoil, we shall take the positive sign in the expression for w. Similarly, we take the initial value of the Mach angle ϕ to be the linear value given by neglecting w $(= O(\epsilon))$ in (4.4), i.e.,

$$\phi(\xi, t = -\xi) = \sin^{-1} \frac{1}{(\dot{X}_0^2 + \dot{Y}_0^2)^{1/2}} = \phi_0(\xi), \text{ say,}$$

so that, neglecting ϕ_1 in comparison with ϕ, we get

$$\theta(\xi, -\xi) = \pi/2 - (\phi - \phi_1) + \psi \approx \pi/2 - \phi_0 + \psi = \theta_0, \text{ say.} \quad (4.12)$$

Using the value ϕ_0 of angle ϕ at P_ζ we get the value g_0 of g from (4.5). Finally, the value of m at $\xi = -t$ is obtained from (3.4).

We have now completed setting up the Cauchy problem on the line $\xi + t = 0$ for each of the one-parameter family of nonlinear wavefronts $\Omega_t^{(\zeta)}$. This is depicted in figure 4.2 where

$$m_0(\xi) = 1 - \frac{(\gamma + 1)(\dot{X}_0^2 + \dot{Y}_0^2) b_u'(\zeta)}{2(\dot{X}_0^2 + \dot{Y}_0^2 - 1)^{1/2}}, \quad (4.13)$$

$$g_0(\xi) = (\dot{X}_0^2 + \dot{Y}_0^2 - 1)^{1/2}, \tag{4.14}$$

$$\theta_0 = \frac{\pi}{2} + \psi - \sin^{-1}\left(\frac{1}{(\dot{X}_0^2 + \dot{Y}_0^2)^{1/2}}\right). \tag{4.15}$$

Let us derive the Cauchy data on the line $\xi + t = 0$ for the system of equations (3.8)–(3.10) governing the propagation of the LS and the TS. For this we shall need the results we have derived for the nonlinear wavefront $\Omega_t^{(\zeta)}$ immediately behind the LS (i.e., ζ very close to 0) and also immediately ahead of the TS (i.e., very close to $-d$). We have denoted the unit normal of the LS or TS by $\mathbf{N}$.

Let us first take up the trailing shock TS. Let Φ be its Mach angle i.e., the angle which this shock makes with the stream line. Consider a figure similar to figure 4.1 with ϕ replaced by Φ, then since M is given by (3.7), Φ at $P_{(-d)}$ is given by (see derivation of (4.4))

$$\sin\Phi = \frac{1 + (\gamma+1)w/4}{\dot{X}_0^2 + \dot{Y}_0^2}. \tag{4.16}$$

It is simple to show that at $P_{(-d)}$,

$$\phi - \Phi \simeq 0(w) = O(\epsilon). \tag{4.17}$$

The normal $\mathbf{N} = (\cos\Theta, \sin\Theta)$ of the TS is given by

$$\Theta = \frac{\pi}{2} - (\Phi - \phi_1) + \psi = \frac{\pi}{2} - (\phi - \phi_1) + \psi + (\phi - \Phi) = \theta + (\phi - \Phi). \tag{4.18}$$

Following the procedure of the derivation of (4.5), we can show that the value of the metric $G(\xi, t)$ on $\xi + t = 0$ is

$$G(\xi, t = -\xi) = \sqrt{\dot{X}_0^{\,2} + \dot{Y}_0^{\,2}}\cos(\Phi - \phi_1) = G_0(\xi), \text{ say.} \tag{4.19}$$

The value of w just ahead of the TS (for the LS it would be the value just behind it) is given by (4.11). The results (4.17) and (4.18) show that up to the first order terms, we can replace θ at $P_{(-d)}$ by Θ, so that the perturbations of the (non-dimensional) flow variables ahead of the TS: $\Omega_t^{(-d)}$ is given, up to order ϵ, by

$$\rho = 1 + w, \ \mathbf{q} = (N_1 w, N_2 w), \ p = \frac{1}{\gamma} + w. \tag{4.20}$$

Substituting this in the boundary condition (4.3) at a point P_ζ on the aerofoil but close to $\Omega_t^{(-d)}$, we get the expression for the shock amplitude similar to (4.9) with ϕ replaced with Φ on the boundary point P_ζ. The Cauchy data $w(\xi, t = -\xi) \equiv w_0(\xi)$ for a nonlinear wavefront can also be treated as a function $w(\zeta, t)$ given by

$$\begin{aligned} w_0(\xi) = w(\zeta, t) &:= w(p, q, t), \ p = \zeta + \mathcal{X}_0(t), \\ q &= b_u(\zeta) + \mathcal{Y}_0(t), \ -d \le \zeta \le 0, \end{aligned} \tag{4.21}$$

where $\mathcal{X}_0$ and $\mathcal{Y}_0$ are given by (2.4) and we remind that $(\mathcal{X}_0, \mathcal{Y}_0)$ are the coordinates of the leading edge of the aerofoil in a frame in which x-axis is parallel to the x'-axis. Note also

that $\psi(t)$ depends on t. Hence, we can write (4.11) in the form

$$w(p,q,t) = -\frac{(\dot{X}_0^2 + \dot{Y}_0^2) b_u'(\zeta)}{\sqrt{\dot{X}_0^2 + \dot{Y}_0^2 - 1}}, \quad -d \le \zeta \le 0. \tag{4.22}$$

Now, we proceed to derive the Cauchy data for V on $\xi + t = 0$. We shall like to differentiate (4.22) once with respect to t and in the next step with respect to ζ. Differentiation with respect to t will give terms w_t, $\dot{\mathcal{X}}_0(t)$ and $\dot{\mathcal{Y}}_0(t)$. We now recall Assumption A3 i.e., the camber length of the aerofoil is small compared to the radius of curvature of the path of the aerofoil. Under this assumption, for the consideration of the relation (4.22) on the boundary of the aerofoil, the path of the leading edge may be taken to be a straight line with the aerofoil instantaneously aligned along the tangent to the path. This implies that we may treat $\dot{\mathcal{Y}}_0(t)/\dot{\mathcal{X}}_0(t)$ to be small of the $O(\epsilon)$ or less. Differentiating (4.22) with respect to t and neglecting $\dot{\mathcal{Y}}_0(t)$ in comparison with $\dot{\mathcal{X}}_0(t)$ on the left-hand side of the result, we get

$$w_t + w_p \dot{\mathcal{X}}_0(t) = -\frac{(\dot{X}_0^2 + \dot{Y}_0^2 - 2)(\dot{X}_0 \ddot{X}_0 + \dot{Y} \ddot{Y}_0)}{(\dot{X}_0^2 + \dot{Y}_0^2 - 1)^{3/2}} b_u'(\zeta). \tag{4.23}$$

Differentiating (4.22) with respect to ζ and neglecting this time the term containing $b_u'(\zeta)$ on the left-hand side (so that w_q term again disappears), we get

$$w_p = -\frac{(\dot{X}_0^2 + \dot{Y}_0^2) b_u''(\zeta)}{(\dot{X}_0^2 + \dot{Y}_0^2 - 1)^{1/2}}. \tag{4.24}$$

Eliminating w_p from (4.23) and (4.24), we get

$$\begin{aligned} w_t &= \frac{(\dot{X}_0^2 + \dot{Y}_0^2) b_u''(\zeta)}{(\dot{X}_0^2 + \dot{Y}_0^2 - 1)^{1/2}} \{\dot{\mathcal{X}}_0(t)\} - \frac{(\dot{X}_0^2 + \dot{Y}_0^2 - 2)(\dot{X}_0 \ddot{X}_0 + \dot{Y} \ddot{Y}_0)}{(\dot{X}_0^2 + \dot{Y}_0^2 - 1)^{3/2}} b_u'(\zeta) \\ &=: \mathcal{F}(\zeta, t), \text{ say, } -d \le \zeta \le 0, \end{aligned} \tag{4.25}$$

where we note that $\dot{\mathcal{X}}_0(t)$ has been put in a curly bracket – it has a special significance as it represents approximately the component of the velocity of the aerofoil in a direction tangential to the path of the aerofoil. In (4.25) both $b_u'(\zeta)$ and $b_u''(\zeta)$ are small and of the same order

$$b_u'(\zeta) = O(\epsilon) = b_u''(\zeta), \quad -d \le \zeta \le 0, \tag{4.26}$$

so that $\mathcal{F}(\zeta, t) = O(\epsilon)$.

We note that up to first order terms (in replacing θ by Θ), the transport equation (6.1.3) of [11], on the nonlinear wavefront just ahead of the shock $\Omega_t^{(-d)}$ can be written as

$$\frac{\partial w}{\partial t} + \left(1 + \frac{\gamma + 1}{2} w\right) \langle \mathbf{N}, \nabla \rangle w = \Omega w, \tag{4.27}$$

where Ω is now the mean curvature of the nonlinear wavefront just ahead of the shock and $\epsilon \tilde{w}$ of (6.1.3) of [11] is w in this paper. This equation is equivalent to equation (10.1.4) of [11] (eq. (10.1.4) is not correctly printed, see eq. (10.1.7) or see eq. (2.5) of [8]).

Equation (4.27) is valid in the interior of the flow on the nonlinear wavefront $\Omega_t^{(\zeta)}$, which meets the boundary of the aerofoil at a point P_ζ. The relation (4.25) is valid at this point

of the boundary. Taking first the limit of (4.27) as we move along $\Omega_t^{(\zeta)}$ to P_ζ, eliminating w_t with the help of (4.25) and finally taking the limit as $\zeta \to -d$, we get

$$V(\xi, t = -\xi) = \frac{\gamma + 1}{4\left(1 + \frac{\gamma+1}{2} w(-d, t)\right)} \{\Omega_{P_{(-d)}} w(-d, t) - \mathcal{F}(-d, t)\}, \tag{4.28}$$

where the quantity V has been defined by (3.11),

$\Omega_{P_{(-d)}}$ = curvature at the trailing end $P_{(-d)}$ of the nonlinear wavefront emanating from that point,

$w(t, -d)$ = value of the amplitude of the perturbation at the trailing end $\equiv w_0(\xi)$ there.

Thus, the value $V_0^{(-d)}(\xi) = V^{(-d)}(\xi, t = -\xi)$ on the Cauchy line $\xi + t = 0$ is obtained, provided we can calculate the curvature $\Omega_{P_{(-d)}}$ of the nonlinear wavefront at the trailing end. We now give a formula for $\Omega_{P_{(-d)}}$.

The expression for $\Omega_{P_{(-d)}}$, namely $-\frac{1}{2}\langle \nabla, \mathbf{n} \rangle$ in terms of θ becomes

$$\Omega_{P_{(-d)}} = -\frac{1}{2g} \frac{\partial \theta}{\partial \xi}. \tag{4.29}$$

To calculate the value of the expression on the right, we use figure 3.1 and the definition (3.2). Then with infinitesimal BC as the directed line segment $= g\delta\xi = g(t - \eta) > 0$ we get

$$\frac{\partial \theta}{g \partial \xi} = \lim_{\delta\xi \to 0} \frac{\theta_C - \theta_B}{BC} = \lim_{\eta \to t} \frac{\theta_C - \theta_B}{g(t - \eta)}. \tag{4.30}$$

Before we use this result, we need to do some intermediate steps. The expression (4.22) at a point P_ζ on the surface of the aerofoil is rewritten as

$$w(\xi, t = -\xi) = w(\xi = -t, t) = -\frac{(\dot{X}_0^2 + \dot{Y}_0^2) b'(\zeta)}{\sqrt{\dot{X}_0^2 + \dot{Y}_0^2 - 1}}, \tag{4.31}$$

which gives $\frac{\mathrm{d}w}{\mathrm{d}\xi}\big|_{\xi=-t} = w_\xi - w_t = \frac{\mathrm{d}w}{\mathrm{d}t}\big|_{\xi=-t}$ so that

$$w_\xi - w_t = \frac{(\dot{X}_0^2 + \dot{Y}_0^2 - 2)(\dot{X}_0 \ddot{X}_0 + \dot{Y} \ddot{Y}_0)}{(\dot{X}_0^2 + \dot{Y}_0^2 - 1)^{3/2}} b'_u(\zeta) =: -\mathcal{F}_1(\zeta, t). \tag{4.32}$$

w_t appearing in (4.32) is the derivative of $w(\xi, t)$ at $\xi =$ constant and is, according to our definition, the rate of change along a ray, i.e., the whole expression on the left-hand side of (4.27) with **N** replaced by **n**. Hence, $w_t = \Omega_{P_{(-d)}} w$, so that (4.32) gives

$$w_\xi\big|_{t=\text{constant}} = \Omega_{P_{(-d)}} w - \mathcal{F}_1(\zeta, t). \tag{4.33}$$

From (3.5) we can obtain an evolution equation for θ in the form $\theta_t = -m_\xi / g$, which with the help of (3.4) and (4.33) gives on the line $\xi = t$,

$$\theta_t = -\frac{\gamma + 1}{2g} w_\xi = -\frac{\gamma + 1}{2g} \{\Omega_{P_{(-d)}} w - \mathcal{F}_1(\zeta, t)\}. \tag{4.34}$$

For an infinitesimal increment $t-\eta$ we get $\theta_C-\theta_A \approx \theta_t|_A(t-\eta)$ so that from (4.29) and (4.30), we have

$$\begin{aligned}\Omega_{P_{(-d)}} &\approx -\frac{1}{2g}\frac{\theta_C-\theta_B}{t-\eta}\\ &= \frac{1}{2g}\left\{\frac{\theta_B-\theta_A}{t-\eta}-\frac{\theta_C-\theta_A}{t-\eta}\right\}\\ &= \frac{1}{2g}\frac{\theta_B-\theta_A}{t-\eta}-\frac{1}{2g}\theta_t\\ &= \frac{1}{2g}\frac{\theta_B-\theta_A}{t-\eta}+\frac{\gamma+1}{4g^2}\{\Omega_{P_{(-d)}}w-\mathcal{F}_1(\zeta,t)\},\quad \text{from (4.34).}\end{aligned} \tag{4.35}$$

The expression on the right-side of (4.35) is split into two terms. Since both w and $\mathcal{F}_1$ are of the order ϵ, the second term is of $O(\epsilon)$. We now examine the first term.

Note that $\theta=\frac{\pi}{2}-(\phi-\phi_1)+\psi$. Since, the point $\zeta=-d$ on the profile is kept fixed, we have $\phi_{1A}=\phi_{1B}$ and

$$\theta_B-\theta_A=-(\phi_B-\phi_A)+\psi_B-\psi_A. \tag{4.36}$$

Since, $\sin\psi=\dot{Y}_0/\dot{X}_0$, $\psi_B-\psi_A=(\dot{X}_0\ddot{Y}_0-\dot{Y}_0\ddot{X}_0)(t-\eta)/\dot{X}_0^2$, for small $t-\eta$. Retaining only the terms up to order one in (4.4), we get $\sin\phi=1/(\dot{X}_0^2+\dot{Y}_0^2)^{1/2}$, so that

$$\phi_B-\phi_A=-\frac{(\dot{X}_0\ddot{X}_0+\dot{Y}_0\ddot{Y}_0)}{(\dot{X}_0^2+\dot{Y}_0^2)(\dot{X}_0^2+\dot{Y}_0^2-1)^{1/2}}(t-\eta). \tag{4.37}$$

When we substitute these values for the expression for $\theta_B-\theta_A$ in (4.36), we note that $(\theta_B-\theta_A)/(t-\eta)$ is of order one so that the first term on the right-hand side of (4.35) is $O(1)$. Hence, retaining only the most dominant terms in (4.35), we finally get

$$\Omega_{P_{(-d)}}=\frac{(\dot{X}_0\ddot{X}_0+\dot{Y}_0\ddot{Y}_0)}{2g(\dot{X}_0^2+\dot{Y}_0^2)(\dot{X}_0^2+\dot{Y}_0^2-1)^{1/2}}+\frac{\dot{X}_0\ddot{Y}_0-\dot{Y}_0\ddot{X}_0}{g\ddot{X}_0^2}. \tag{4.38}$$

In (4.28), $w(-d,t)$ and $\mathcal{F}(-d,t)$ are both of order ϵ and in the denominator on the right-hand side we may neglect $(\gamma+1)w(-d,t)/2$ and finally we get

$$V_0^{(-d)}(\xi)=\frac{\gamma+1}{4}\{\Omega_{P_{(-d)}}w(-d,t)-\mathcal{F}(-d,t)\}, \tag{4.39}$$

where $\Omega_{P_{(-d)}}$ is given by (4.38) and $\mathcal{F}(-d,t)$ is given by (4.25).

Collecting all these results, we write the Cauchy data on the line $\xi+t=0$ for the system (3.8)–(3.10) here.

$$M(\xi,-\xi)=M_0(\xi):=1-\frac{(\gamma+1)(\dot{X}_0^2+\dot{Y}_0^2)b_u'(\xi)}{4(\dot{X}_0^2+\dot{Y}_0^2-1)^{\frac{1}{2}}}, \tag{4.40}$$

$$G(\xi,-\xi)=G_0(\xi):=(\dot{X}_0^2+\dot{Y}_0^2-1)^{\frac{1}{2}}, \tag{4.41}$$

$$\Theta(\xi,-\xi)=\Theta_0(\xi):=\frac{\pi}{2}+\psi-\sin^{-1}\{1/(\dot{X}_0^2+\dot{Y}_0^2)^{\frac{1}{2}}\}, \tag{4.42}$$

$$V(\xi, -\xi) = V_0(\xi) := \frac{\gamma+1}{4}\{\Omega_{p_{(-d)}} w_0(\xi) - \mathcal{F}(-d, t)\}, \tag{4.43}$$

where

$$\Omega_{P_{(-d)}} = \frac{(\dot{X}_0\ddot{X}_0 + \dot{Y}_0\ddot{Y}_0)}{2g(\dot{X}_0^2+\dot{Y}_0^2)(\dot{X}_0^2+\dot{Y}_0^2-1)^{1/2}} + \frac{\dot{X}_0\ddot{Y}_0 - \dot{Y}_0\ddot{X}_0}{g\ddot{X}_0^2},$$

$$\mathcal{F}(\zeta, t) = \frac{(\dot{X}_0^2+\dot{Y}_0^2)b_u''(\zeta)}{(\dot{X}_0^2+\dot{Y}_0^2-1)^{1/2}}\{\dot{\mathcal{X}}_0(t)\} - \frac{(\dot{X}_0^2+\dot{Y}_0^2-2)(\dot{X}_0\ddot{X}_0+\dot{Y}\ddot{Y}_0)}{(\dot{X}_0^2+\dot{Y}_0^2-1)^{3/2}} b_u'(\zeta),$$

$$\mathcal{X} = X_0\cos\psi + Y_0\sin\psi.$$

5. Discussion on the hyperbolic and elliptic nature of the equations governing the evolution of $\Omega_t^{(\zeta)}$

Let us first start with the eqs (3.5) and (3.6) for $-d < \zeta < 0$, $\zeta \neq G$. The expression (4.13) for the value of m at P_ζ at a time t gives valuable information about the nature of the equations (3.5) and (3.6). The Mach angle ϕ is defined for values of the aerofoil speed $(\dot{X}^2+\dot{Y}^2)^{1/2} \geq 1+((\gamma+1)/2)w$ and since $|w| \ll 1$, the right-hand side is approximately equal to 1. In any case $0 < \phi < \pi/2$. For simple aerofoil, $b_u(\zeta)$ has its maximum at just one point $\zeta = G$, $-d \leq G \leq 0$ and we assume that the aerofoil has non-zero angles at the leading and trailing edges. This means

$$b_u'(G) = 0, b_u'(\zeta) > 0 \text{ for } -d \leq \zeta < G,\ b_u'(\zeta) < 0 \text{ for } G < \zeta \leq 0. \tag{5.1}$$

This justifies the negative sign in the beginning of the expression in (4.11) since w should be positive in $G < \zeta < 0$ and negative when $-d < \zeta < -G$.

Equation (4.11) or (4.13) now implies that (see figure 2.2)

$$w > 0 \text{ i.e., } m > 1 \text{ at } P_\zeta \text{ for } G < \zeta \leq 0, \tag{5.2}$$

$$w < 0 \text{ i.e., } m < 1 \text{ at } P_\zeta \text{ for } -d \leq \zeta < G, \tag{5.3}$$

$$w(P_G) = 0 \text{ i.e., } m(P_G) = 1. \tag{5.4}$$

Thus, we are able to determine the sign of w or $m-1$ at a point P_ζ where the nonlinear wavefront $\Omega_t^{(\zeta)}$ meets the surface of the aerofoil. Is the sign of the amplitude w same on all points of $\Omega_t^{(\zeta)}$? We discuss it in the next paragraph based on our experience with computational results.

What should be the sign of $m-1$ on the whole wavefront $\Omega_t^{(\zeta)}$ for a given ζ? There are two ways to get the answer. The first way is based on experimental results or observation. The sonic boom, as depicted in figure 2.1, is bounded by a LS, through which the gas is compressed and hence $w > 0$ behind this shock i.e., $M-1 > 0$ on it, and a TS through which an expanded gas is compressed to the normal atmospheric pressure and hence $w < 0$ ahead of this shock i.e., $M-1 < 0$ on it. The value of $m-1$ on a nonlinear wavefront which interact the LS or TS, is related to the value $M-1$ through the relations (3.4) and (3.7). Thus, for $G < \zeta < 0$, $m-1 > 0$ not only at the base point P_ζ of $\Omega_t^{(\zeta)}$, but also at the point where $\Omega_t^{(\zeta)}$ interacts with the LS. If we assume (following some experimental results) that the variation of w or $m-1$ across a sonic boom at any time has an N-wave

or U-wave shape (see figure 4 of [10]), then there is only one curve in between the two shocks where $m = 1$ and which does not intersect with the LS and the TS. This curve, therefore must be a linear wavefront as depicted in figure 2.1 by the line $\Omega_t^{(G)}$. On the nonlinear wavefronts between the linear wavefront and LS we must have $m - 1 > 0$ and on those between the linear wavefront and TS we must have $m - 1 < 0$.

The second way is purely mathematical. For this, we need to go back to figure 4.2. For a fixed point P_ζ, ($\zeta \neq G$) on the aerofoil i.e., for a given ζ, $m_0(\xi) - 1$ is either greater than or less than zero on the whole Cauchy line $\xi + t = 0$. From the full Cauchy data i.e., the values of $m_0(\xi)$, $\theta_0(\xi)$ and $g_0(\xi)$ as given in (4.13)–(4.15) and the conservation laws (3.5) and (3.6), it should be possible to determine the sign of $m - 1$ in the half plane $\xi + t > 0$. We have not been able to do this, but we believe that $m_0(\xi) - 1 > 0$ or $m_0(\xi) - 1 < 0$ on $\xi + t = 0$ would imply $m - 1 > 0$ or $m - 1 < 0$ respectively. Our extensive numerical computation with $m - 1 > 0$ reported in our previous publications does indicate that if $m_0(\xi) - 1 > 0$ at any point P of a nonlinear ray, then $m - 1 > 0$ at all points of the ray. Therefore, it should be possible to prove that for the Cauchy problem in figure 4.2, $m_0 - 1 > 0$ on the line $\xi + t = 0$ would imply $m - 1 > 0$ at all the points on any horizontal line $\xi =$ constant on the right side of the Cauchy line. We give below only a convincing argument based on the assumption that the mean curvature Ω of $\Omega_t^{(\zeta)}$ does not tend to infinity along a ray. We have found this assumption to be true in our previous theoretical and computational results for $m - 1 > 0$ where caustic type of singularities on a linear wavefront are resolved into kinks on the corresponding nonlinear wavefront.

Let us further discuss the case $m - 1 > 0$. We first note that when we follow a ray, $g = (x_\xi^2 + y_\xi^2)^{1/2}$ vanishes at a point where the ray meets a caustic. But a caustic type of singularity does not appear on a nonlinear wavefront for $m - 1 > 0$ so that g does not vanish on a nonlinear ray. Integrating the ray equation (3.6) with respect to t (or taking its jump across a kink path), we get

$$g(m-1)^2 \mathrm{e}^{2(m-1)} = g_0(m_0-1)^2 \mathrm{e}^{2(m_0-1)}, \tag{5.5}$$

which shows that m does not tend to infinity along a ray. Our computational results also show that m always remains bounded. From the equations (3.5) and (3.6), we can deduce a transport equation for w along a ray

$$\frac{\mathrm{d}w}{\mathrm{d}t} = \Omega w \tag{5.6}$$

(see equation (6.1.3) of [11]; or equation (2.5) of [8]). Integrating along the ray, we get

$$w = w_0 \mathrm{e}^{\int_\eta^t \Omega(\tau)\mathrm{d}\tau}, \quad w(t) = w_0, \tag{5.7}$$

which shows that w retains the same sign as long as the mean curvature Ω of $\Omega_t^{(\zeta)}$ does not tend to $-\infty$. The case $\Omega < 0$ corresponds to a wavefront convex to the state ahead of it and hence the case Ω tending to $-\infty$ cannot arise as long as the rays keeps on diverging. The divergence of rays is ultimately arrested (except in the case of circular symmetric shape and uniform distribution of the amplitude on the wavefront at any time t) and they tend to become parallel as seen in figure 10.3.11 of [11]* and figure 5 of [2] so that magnitude of Ω actually decreases. As seen in figure 10.3.4 of [11], when the initial wavefront has a

*Note that figures 10.3.4, 10.3.9, 10.3.10 and 10.3.11 of [11] has been reproduced from figures 5, 10, 11 and 12 of [8].

concave part (with $\Omega > 0$) and a convex part (with $\Omega < 0$), the diverging rays from the convex part are usually pushed and start converging but even then the magnitude of the curvature keeps on decreasing. Also, as seen in figures 10.3.4, 10.3.9 and 10.3.10 of [11], the converging rays from the concave part of a nonlinear wavefront (or shock front) are prevented from focusing by appearance of kinks and Ω tending to $+\infty$ on a ray is always avoided. There are many other numerical results in these papers, the results always show that the magnitude of the curvature of a nonlinear wavefront along a ray keeps on decreasing as time passes and never tends to infinity. Hence w given by (5.7) always remains bounded and maintains the same sign so that $m > 1$.

At present, we do not have a very clear idea of the nature of singularities which appear on $\Omega_t^{(\zeta)}$ when $w < 0$ i.e. $m - 1 < 1$. However, we shall see that when $w < 0$ on $\Omega_t^{(\zeta)}$, eqs (3.5) and (3.6) governing the evolution of $\Omega_t^{(\zeta)}$ is elliptic and hence θ and g are expected to remain smooth functions of ξ and t so that $\Omega_t^{(\zeta)}$ is kink-free. In this case, based only on experimental results, we assume that w retains the same sign on a ray as w_0 at P_ζ. This assumption requires a mathematical proof or at least is to be checked from computation. The discussion so far leads to a conclusion that the model of the sonic boom which we have proposed is consistent in every respect and it is generated by one-parameter family of nonlinear wavefronts $\Omega_t^{(\zeta)}$ such that $m > 1$ for $G < \zeta < 1$ and $m < 1$ for $-d < \zeta < 1$ and these nonlinear wavefronts are bounded by LS with $M > 1$ and TS with $M < 1$.

The eigenvalues of the system (3.5) and (3.6) are

$$\lambda_1 = -\sqrt{\frac{m-1}{2g^2}},\ \lambda_2 = 0,\ \lambda_3 = \sqrt{\frac{m-1}{2g^2}}. \tag{5.8}$$

Similarly, the eigenvalues of the systems (3.8)–(3.10) are

$$\Lambda_1 = -\sqrt{\frac{M-1}{2G^2}},\ \Lambda_{11} = \Lambda_{12} = 0,\ \Lambda_3 = \sqrt{\frac{M-1}{2G^2}}. \tag{5.9}$$

There exist two linearly independent eigenvectors corresponding to the double eigenvalue 0 in (5.9).

Since, $m > 1$ on each of the nonlinear wavefronts $\Omega_t^{(\zeta)}$, $G < \zeta < 0$ and $M > 1$ on the leading shock front $\Omega_t^{(0)}$, the systems of conservation laws (3.5) and (3.6) and (3.8)–(3.10) governing them are hyperbolic. As seen in our earlier work, these nonlinear wavefronts and the LS may develop kinks. In fact, in the case of the motion of an accelerating aerofoil on a straight path (say, along the x-axis), the linear wavefronts are concave to the medium ahead and develop a caustic as in figure 5.1, where we have shown the linear wavefront from the leading edge i.e., from $\zeta = 0$. In the same figure, we have also shown the nonlinear wavefront from the leading edge $\zeta = 0$ and note the qualitative difference in its shape, the nonlinear wavefront does not have a fold: a pair of cusp type of singularities on the linear wavefront are replaced by a pair of kinks on the nonlinear wavefront. When the aerofoil moves with a constant speed on a curved path, say concave downwards, then the wavefronts from the points on the upper surface of the aerofoil remain smooth for all time, whereas those wavefronts from the lower surface of the aerofoil develop a pair of kinks. These results are depicted in figure 5.2. In figure 5.3, we have shown details of the wavefronts from the leading edge in the focused region from the lower surface of the aerofoil at time $t = 5$. Since, the wavefronts are concave to the medium ahead, the one from the linear ray theory develops a cusp type of singularity and the wavefront from

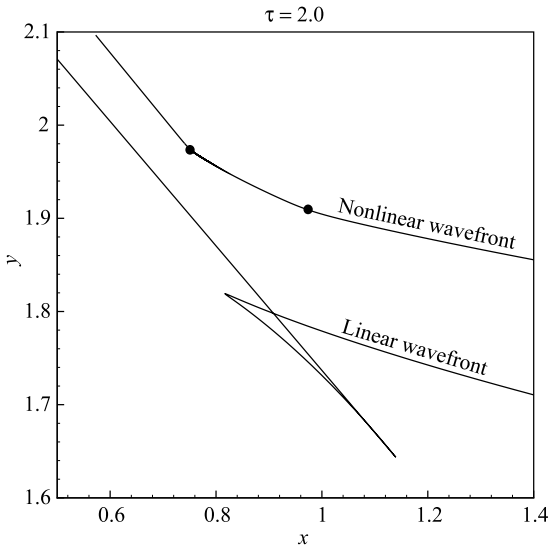

Figure 5.1. Sonic boom wavefront at $t = 2$ from the leading edge of an accelerating aerofoil moving in a straight path. Kinks on the nonlinear wavefront are shown by dots. The initial Mach number is 1.8 and the acceleration is 10 in the time interval $(0, 1/2)$.

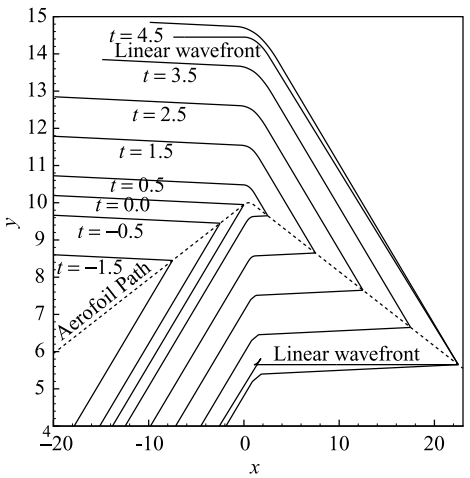

Figure 5.2. The nonlinear wavefront from the leading edge of an aerofoil moving with a constant Mach number 5 along a path concave downwards with $b'_u(0) = -0.01$.

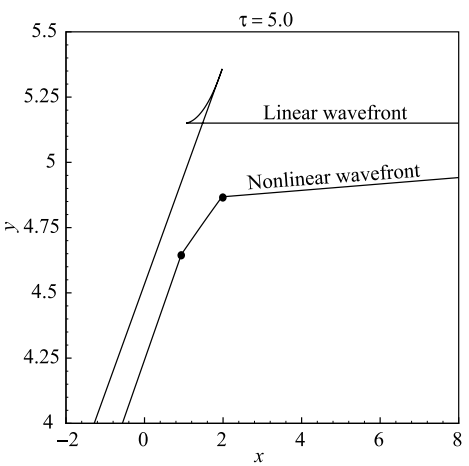

Figure 5.3. Linear and nonlinear wavefronts in the case of figure 5.2 at $t = 5$.

WNLRT develops a pair of kinks as seen in the figure. As in our previous investigation [2], we expect the LS: $\Omega_t^{(0)}$ to have the same shape as that of the nonlinear wavefront. In fact, some preliminary computation of $\Omega_t^{(0)}$ by SRT has already shown that $\Omega_t^{(0)}$ is very close to the nonlinear wavefront from the leading edge. We shall report the exact results of our extensive numerical computation in future publications. It is very interesting to note

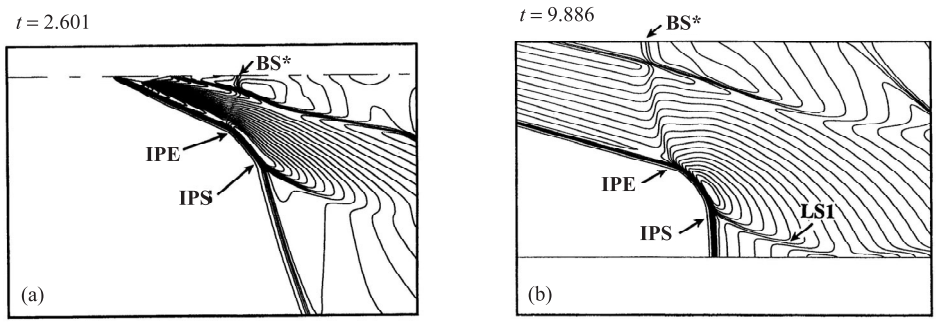

Figure 5.4a, b. Numerical solutions of Euler equations for the flow over a diamond-shaped aerofoil moving from right to left with Mach number starting from 1.2 to 4. The figures are reproduced from [5] with the permission of the authors.

that similar results have been obtained from a limited (due to limited choice of parameters to imitate a sonic boom problem) numerical computation of the full Euler's equations by Inoue, Sakai and Nishida [5]. Some of their results have been reproduced in figures 5.4 and 5.5.

The aerofoil in figure 5.4a is moving from left to right and accelerates from a Mach number 1.2 to 4.0. The figure depicts the boom produced by the lower surface of a diamond-shaped aerofoil. We note that the leading shock (LS) tends to focus and develops two kinks (marked in the figure by IPE and IPS).

Since $m-1 < 0$ on each of the nonlinear wavefront $\Omega_t^{(\zeta)}$ $(-d < \zeta < G)$ and $M-1 < 0$ on the trailing shock $\Omega_t^{(-d)}$, the pair of eigenvalues (λ_1, λ_3) and (Λ_1, Λ_3) are purely imaginary. The systems (3.5) and (3.6) and (3.8)–(3.10) are no longer hyperbolic. In fact, for the two important modes corresponding to the eigenvalues (λ_1, λ_3) and (Λ_1, Λ_3) respectively, the two systems have the same nature as that of an elliptic equation. We may think that $M < 1$ for the TS is physically unrealistic but this is not so because the trailing shock is moving not into the undisturbed gas with $(\rho = \rho_0,\ \mathbf{q} = 0,\ p = p_0)$ but into a gas which has already gone through an expansion phase between $-d < \zeta < G$. The actual Mach number of the TS is M_{TS}

$$M_{\mathrm{TS}} = \left.\frac{M-1-(m-1)}{|m-1|}\right|_{\mathrm{TS}} = \left.-\frac{\gamma+1}{4|m-1|}w\right|_{\mathrm{TS}} > 0, \tag{5.10}$$

since $w|_{\mathrm{TS}} = w(-d, t) < 0$. We can easily verify that the TS satisfies Lax's entropy condition

$$\left(1+\frac{\gamma+1}{2}w\right) < \left(1+\frac{\gamma+1}{4}w\right) < 1 \tag{5.11}$$

since w here is $w|_{\mathrm{TS}} < 0$.

The elliptic nature (in the modes corresponding to the eigenvalues $\lambda_1, \lambda_3, \Lambda_1$ and Λ_3) of the systems (3.5) and (3.6) for $d < \zeta < G$ and (3.8)–(3.10) for $\zeta = -d$ implies that the systems have no discontinuous solutions in the (ξ, t)-plane which would map on to kinks in the (x, y)-plane and the corresponding curves $\Omega_t^{(\zeta)}$ and $\Omega_t^{(-d)}$ must be free from kinks. Thus, we expect that the trailing shock TS will not develop kinks and will remain smooth. Though a property like smoothness is hard to see in and predict from a numerical result,

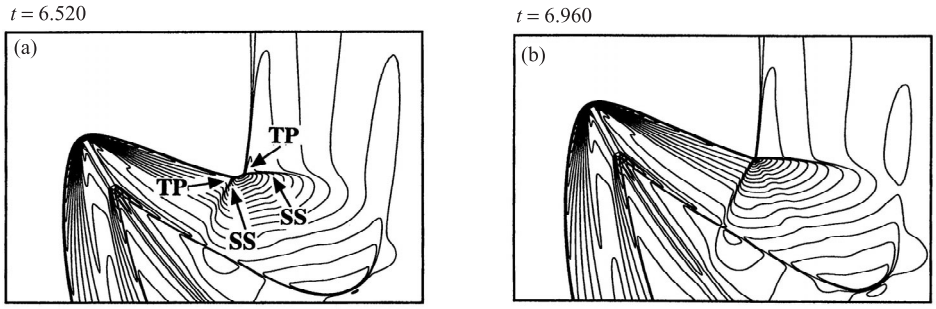

Figure 5.5a, b. The flow produced by a blunt body on a curved path. We find in the upper part a LS with two kinks (denoted by TP) and a TS which is smooth. In the lower part we find a LS which is curved upward and smooth as far as we can see. The figures are reproduced from [5] with the permission of the authors.

especially from the numerical solution of Euler's equations, we note that figures 5.4a and 5.4b show the trailing shock to be smooth. This is in spite of the fact that the Mach stems (one from IPE as seen in figure 5.4b) from LS come and interact with the TS. Formation of kinks IPE and IPS on the LS follows from the results of our previous papers (since LS is concave) but *smoothness of the TS is a surprising new result which we conjecture in this paper and this requires a deeper investigation and a mathematical proof.* In figure 5.5 we reproduce another result of Inoue, Sakai and Nishida [5]. Though the flow in this case is produced by a blunt body, it illuminates the most important part of our theory. The LS in the upper part (the direction in which the flight path is concave) has two kinks (TP). The third shocks from the kinks enter into the disturbed region but seem to become so weak that they hardly affect the TS, which appears to be smooth. The LS in the lower part is convex with respect to the region into which it is propagating and hence it is smooth as far as it is seen and our theory shows that it would not develop kinks. Another interesting result, which we note is that the two kinks of figure 5.5a are about to interact in figure 5.5b. Interaction of kinks (and also *elementary waves*) have been studied in detail by Baskar and Prasad [1]. These two kinks after interaction, will produce another pair of kinks which will start moving apart.

The strength of a convex shock, for which rays diverge, decreases as the shock propagates. Hence the flight of a maneuvering aircraft should be such that it produces a convex shock propagating towards the ground. This means that the path of an accelerating aircraft should curve upward in order to minimize the effect of the boom on the ground. However, extensive calculations for a convex nonlinear wavefront or a shock by our weakly nonlinear ray theory (WNLRT) and shock ray theory (SRT), show that the corrugational stability of the shock (see §§10.3–10.5 of [11] and figure 5 of [2]), which is a nonlinear effect, will intervene and would not allow the shock strength to decay as fast it could have been according to the linear theory. In this case the decay in the shock strength is not due to geometric effect but more due to dissipation of energy (see figure 10.3.11 of [11]). If an aircraft continues to accelerate in a straight path either horizontally or at an angle, say $\pi/6$, the boom produced will be concave downwards as in figures 5.2, 5.3 and 5.4a, and hence will be stronger. Our theory shows that a concave leading shock (LS) does not focus, in this case the caustic having infinite wave intensity is replaced by a pair of kinks in such a way that on all points of the concave shock, the shock strength increases but it remains of the same order of strength as that of the strength of the initial shock produced on the body

of the aircraft. In addition the dissipation through kinks starts dominating and this leads to a decay in the shock strength (see figures 10.4.3 of [11]). Hence, when LS is converging there is no possibility of getting a very strong shock with strength of higher order of magnitude than what is produced. However, the aircraft should avoid producing a concave shock towards the ground.

Acknowledgements

The authors sincerely thank AR & DB, Ministry of Defence, Govt. of India for financial support through the project "Nonlinear hyperbolic waves in multi-dimensions with special reference to sonic booms" (No. DARO/08/1031199/M/I). Phoolan Prasad thanks Alexander Von Humboldt Foundation for providing financial support to work in Germany and Prof. G Warnecke who provided an excellent facility to work in his research group at IAN, Department of Mathematics, University of Magdeburg. S. Baskar thanks the National Board of Higher Mathematics for their financial support as a postdoctoral fellow in the Department of Mathematics, Indian Institute of Science, Bangalore, India.

References

[1] Baskar S and Prasad P, Riemann problem for kinematical conservation laws and geometric features of a nonlinear wavefront, *IMA J. Appl. Maths* **69** (2004) 391–420
[2] Baskar S and Prasad P, Propagation of curved shock fronts using shock ray theory and comparison with other theories, *J. Fluid Mech.* **523** (2005) 171–198
[3] Courant R and Friedrichs K O, Supersonic flow and shock waves (New York: Interscience Publishers) (1948)
[4] Crow S C, Distortion of sonic bangs by atmospheric turbulance, *J. Fluid Mech.* **37** (1969) 529–563, NPL Aero Report 1260
[5] Inoue O, Sakai T and Nishida M, Focusing shock wave generated by an accelerating projectile, *Fluid Dynamics Research* **21** (1997) 403–416
[6] Kevlahan N K R, The propagation of weak shocks in non-uniform flow, *J. Fluid Mech.* **327** (1996) 167–197
[7] Morton K W, Prasad P and Ravindran R, Conservation forms of nonlinear ray equations, Tech. Rep., 2, Dept. of Mathematics, Indian Institute of Science (1992)
[8] Monica A and Prasad P, Propagation of a curved weak shock, *J. Fluid Mech.* **434** (2001) 119–151
[9] Pilon A and Lyrintzis A, A data-parallel TVD method for sonic boom calculations, Preprint 95-003 (Minnesota: University of Minnesota) (1995)
[10] Plotkin K J, State of the art of sonic boom modeling, *J. Acoust. Soc. Am.* **111(1)** (2002) 530–536
[11] Prasad P, Nonlinear hyperbolic waves in multi-dimensions, Chapman and Hall/CRC, Monographs and Surveys in Pure and Applied Mathematics 121, (2001)
[12] Prasad P and Sangeeta K, Numerical simulation of converging nonlinear wavefronts, *J. Fluid Mech.* **385** (1999) 1–20
[13] Whitham G, Linear and nonlinear waves (New York: John Wiley & Sons) (1974)